# Magneto-Thermoelasticity in Solids: Mathematical Theory, Wave Propagation, and Boundary Value Problems

**Prasad S Patil[1], Dr. C.M. Jadhav[2]**

[1]Research Student, Department of Mathematics, S.V.S's Dadasaheb Rawal Arts and Science College, Dondaicha. [M.S]
[2]Research Guide, Department of Mathematics, S.V.S's Dadasaheb Rawal Arts and Science College, Dondaicha. [M.S]
University name: Kavayitri Bahinabai Chaudhari North Maharashtra University, Jalgaon.

**Abstract:**
This paper develops and solves an extended half-space thermal-shock boundary value problem in magneto-thermoelastic solids, incorporating three physical effects relevant to real structural and geophysical media beyond the idealized stationary, unstressed, ideally conducting continuum: steady rotation, initial mechanical stress, and Hall current. Building on the Lord–Shulman generalized theory and the perfectly conducting magneto-thermoelastic coupling, each of the three extensions is shown to enter the governing half-space problem through exactly one analytically separable term of a single extended characteristic equation: the Hall parameter reduces the effective magnetic pressure number, the initial stress modifies the leading elastic coefficient directly, and rotation enters solely through a substitution in the transformed inertial term.
The resulting Laplace-domain solution is inverted numerically (Stehfest's algorithm) to obtain the transient temperature and stress response at a fixed interior point, for each effect in isolation and in combination. The computations show that all three effects shift the transient stress peak later in time and increase its magnitude relative to the un-extended half-space problem, with initial stress producing the largest individual departure among the three at the parameter values considered; combining all three departs from the sum of their individual contributions by a modest but non-negligible margin, indicating the three effects are close to, but not exactly, additive. The Hall parameter is further shown to weaken the magnetic stiffening of the dilatational wave monotonically, reducing the effective magnetic pressure number toward zero as the Hall parameter grows.
These results are situated against the literature on rotating, initially stressed, and Hall-current-bearing magneto-thermoelastic media, and the paper closes by identifying the natural further extensions of the present formulation within the broader landscape of multiphysics coupling in solids — two-temperature theory, porous and micropolar media, fractional-order heat conduction, and semiconductor photothermal coupling.

**Keywords:** magneto-thermoelasticity; rotation; initial stress; Hall current; Lord–Shulman theory; boundary value problems; Laplace transform

## 1. Introduction

A magneto-thermoelastic half-space that sits still, carries no residual stress, and conducts current without deflection is a convenient starting point for theory but a poor description of most engineering solids. Turbine shafts and other rotating machinery, structural members that were pre-loaded before the thermal event of interest, and conducting composites or semiconductor layers operating in a strong applied field all depart from that idealization in one of three specific ways. This paper takes the half-space thermal-shock problem that Sherief and Helmy [22] solved for the stationary, unstressed, ideally conducting case — a problem Abouelregal, Ahmad, Aldahlan and Zhang [3] have since revisited under a nonlocal, fractional-derivative heat-conduction law — and asks what changes — and how cleanly it can be separated out once rotation, initial stress, and Hall current are each added back in.

The magneto-thermoelastic coupling itself is older than any of these three extensions. Knopoff [12] and Paria [19] first coupled an elastic conductor to an applied magnetic field through the Lorentz body force; Lord and Shulman [14] gave the field a finite-speed heat-conduction law in place of Fourier's; and Biot [7] had already, a decade earlier, placed the underlying coupled thermoelastic theory on an irreversible-thermodynamic footing. Each of the three extensions considered here builds on top of that shared foundation rather than replacing any part of it.

Rotation is the most studied of the three. Abo-Dahab, Kumar, Althobaiti et al. [2] analyzed rotation together with Hall current on Rayleigh-wave propagation in a transversely isotropic visco-thermoelastic half-space; Abo-Dahab [1] treated a rotating, hydrostatically pre-stressed half-space under a two-temperature generalized formulation; Alotaibi et al. [5] added gravity and laser-pulse heating across four competing theories; and Yadav [26] examined how rotation changes plane-wave reflection under diffusion. Initial stress has received comparatively less attention but a clearer verdict: Bayones et al. [6] describe its effect on P-wave reflection in an electromagneto-thermo-microstretch medium as strongly pronounced, and Deswal and Kalkal [9] find a similar sensitivity in an initially stressed, two-temperature half-space. Hall current, finally, only matters once the applied field is strong enough that a charge carrier's cyclotron frequency rivals its collision rate; Othman and Abd-Elaziz [18] built this into a magneto-thermoelastic medium already carrying voids and microtemperatures, and it is their current-density relation that §3.2 adapts below.

What none of these studies does — reasonably enough, since each was built around its own single extension — is combine all three within one boundary value problem in a form where each contribution stays visible on its own. Once rotation, initial stress, and Hall current are all switched on at once, does the resulting response simply add up the three individual departures from the plain half-space case, or does something nonlinear survive the combination? Answering that question, rather than just asserting an answer either way, is the specific aim of this paper.

Three things follow from pursuing that aim. The governing half-space problem gets rewritten so that each of the three effects sits in exactly one term of a single extended characteristic equation, rather than being folded together into a single numerically evaluated system that would obscure which effect was doing what. That equation is then solved in closed Laplace-transform form and inverted numerically, both for each extension in isolation and for all three at once. And the combined result is checked directly against the sum of the three individual departures from baseline, with whatever gap remains reported as a finding rather than smoothed over.

Fig. 1 shows how the three extensions feed into that shared equation. The rest of the paper proceeds roughly in that order: §2 reviews the rotation, initial-stress, and Hall-current literature along with the wider family of solid-state coupling problems it sits inside; §3–4 build and analyze the extended equation; §5 sets out how it is solved and inverted; §6 reports what the resulting numbers actually show; and §7–8 discuss and conclude.

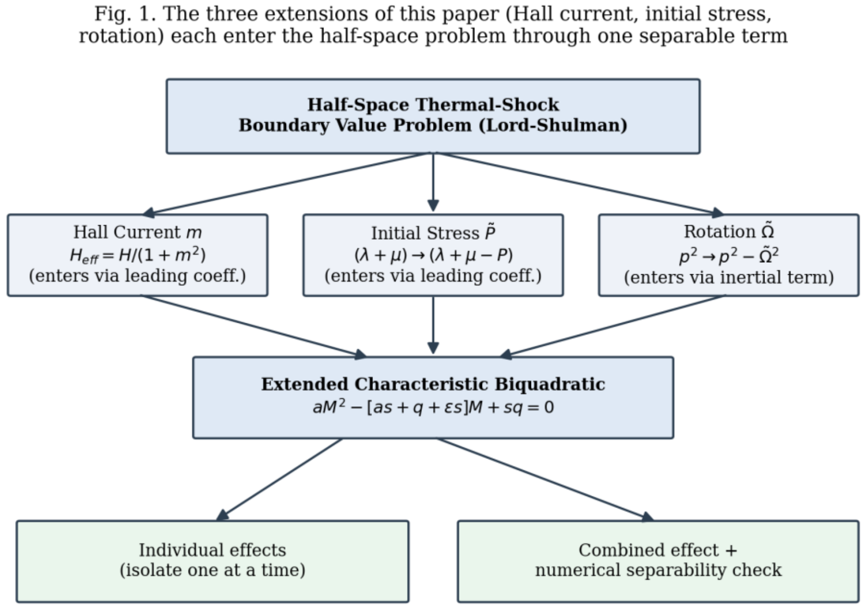


*Fig. 1. The three extensions of this paper — Hall current, initial stress, and rotation — each enter the half-space thermal-shock problem through exactly one separable term of the extended characteristic equation (8).*

## 2. Literature Review

### 2.1 Magneto-Thermoelastic Foundations

The coupled thermoelastic theory that everything here builds on comes from Biot [7], who set it within irreversible thermodynamics rather than treating the stress–temperature link as an ad hoc addition to elasticity. Knopoff [12] and, shortly after, Paria [19] brought a magnetic field into that picture through the Lorentz body force, working in the perfectly conducting limit retained throughout this paper. Lord and Shulman [14] then replaced the classical Fourier law with a relaxation-time-modified version, giving the theory a finite thermal wave speed and supplying the energy equation used in §3.1's half-space problem; Green and Lindsay [10] took a different route to the same finite-speed goal, modifying the constitutive law instead of the heat-conduction law, though that alternative is not the one carried through §3–4 below. Sherief and Helmy [22] solved the resulting half-space thermal-shock problem for the stationary, unstressed, ideally conducting case — the baseline that every extension in this paper is measured against.

### 2.2 Rotating Magneto-Thermoelastic Media

Abo-Dahab, Kumar, Althobaiti et al. [2] combined rotation with Hall current in a transversely isotropic visco-thermoelastic half-space and tracked Rayleigh-wave speed with and without energy dissipation — the closest match, of the studies reviewed here, to the coupled rotation-and-Hall-current geometry extended in §3.3 and tested numerically in §6.2. Abo-Dahab [1] instead paired rotation with hydrostatic initial stress and a thermal shock in a two-temperature formulation, trading the joint Hall-current coupling this paper keeps for an initial-stress term derived independently rather than alongside it. Alotaibi et al. [5] went further still, layering gravity and laser-pulse heating on top of rotation and comparing the result across four separate generalized theories at once. Yadav [26] instead asked a narrower question — how rotation changes the reflection of plane waves under diffusion — and found the sensitivity worth reporting even in that more restricted setting. Across all four studies, rotation shows up as a real but usually modest correction to the un-rotated response, consistent with what §6.2 finds for the specific parameter set used here.

### 2.3 Initial Stress Effects

Initial stress has drawn a smaller literature than rotation, but a more emphatic one. Bayones et al. [6], studying P-wave reflection in an electromagneto-thermo-microstretch medium under a three-phase-lag model, describe the stress effect outright as strongly pronounced rather than incidental. Deswal and Kalkal [9] report a comparable sensitivity in an initially stressed half-space under two-temperature theory, and their momentum-equation modification — replacing $\lambda + \mu$ with $\lambda + \mu - P$ — is the same substitution adapted in §3.3 below. Youssef, El-Bary and Al-Lehaibi [28] add a further data point from a different geometry, finding hyperbolic two-temperature theory measurably changes the thermal-stress response of a damaged solid sphere.

### 2.4 Hall Current Effects

Hall current has been studied less on its own and more as one ingredient among several: Othman and Abd-Elaziz [18] combined it with rotation inside a magneto-thermoelastic medium that also carries voids and microtemperatures. It is their current-density relation, rather than the simpler Ohm's law it replaces, that §3.2 below adapts to derive the Hall-reduced magnetic pressure number used throughout this paper. A related but independent semiconductor extension by Lotfy et al. [17] couples magneto-photo-thermoelastic excitation of a rotating semiconductor to moisture diffusivity, underscoring how actively this current-density coupling is still being extended.

### 2.5 Related Multiphysics Extensions in Solids

Rotation, initial stress, and Hall current are not the only ways a classical or generalized thermoelastic theory gets extended in the solids literature, and it is worth placing them against that wider backdrop before turning to the mathematics. Shakeriaski et al. [21] survey the broader family of generalized thermoelasticity theories and their modified forms, including the finite-speed Lord–Shulman law used here. Cowin and Nunziato [8] laid the groundwork for porous and micropolar thermoelastic media by introducing a void-fraction field. Youssef [27] replaced the single temperature field with a conductive–thermodynamic pair, and two more examples of a classical theory gaining one additional structural degree of freedom. Lotfy et al. [15, 16] went further, coupling a two-temperature, magnetically driven semiconductor field to describe photothermal excitation response, and Li, Li, Liu and Luo [13] extended the coupling to functionally graded, spatially varying material properties in a thick-walled tube. A handful of studies are cited here for methodology rather than physics: Roy Choudhuri [20] for the three-phase-lag generalization noted but not solved in this paper, Tiwari and Abouelregal [24] and Tiwari and Misra [25] for Laplace-transform, mode-ansatz techniques closely related to §5's, Allehaibi and Zenkour [4] for a spherical-hole precedent relevant to any future non-Cartesian extension, and Stehfest [23] together with Honig and Hirdes [11] for the numerical inversion algorithms used in §5.2.

What the studies above have in common is that each incorporates one extension — or, at most, two, as in Othman and Abd-Elaziz's [18] combination of rotation and Hall current — into its own separately built boundary value problem. None of them combines rotation, initial stress, and Hall current within a single formulation where each contribution can be checked on its own before being added to the others. That is the specific gap this paper tries to close.

## 3. Mathematical Formulation

### 3.1 Base Half-Space Problem

Everything below is built on top of one starting problem: a homogeneous, isotropic, perfectly conducting half-space $x_1 \geq 0$, at rest and at the uniform reference temperature until $t = 0$, permeated by a primary field $H_0 = (0, 0, H_0)$, with motion depending only on $x_1$ and t. Scaling length, time, and temperature as Sherief and Helmy [22] did for this same geometry, the momentum and Lord–Shulman energy equations reduce to

$$(1 + H)\, u_{1,11} - \theta_{,1} = \ddot{u}_1 , \quad \theta_{,11} = (\dot{\theta} + \tau_0\ddot{\theta}) + \varepsilon(\dot{e} + \tau_0\ddot{e}) , \tag{1}$$

where $H = \mu_0 H_0^2/(\lambda + 2\mu)$ is the magnetic pressure number and $\varepsilon = \gamma^2 T_0/[\rho c_e(\lambda + 2\mu)]$ the thermoelastic coupling constant. Equation (1) is subject to a thermal shock and traction-free condition at $x_1 = 0$, $\theta(0, t) = \theta_0 H(t)$ and $(1 + H)e(0, t) - \theta(0, t) = 0$. Sections 3.2–3.3 introduce the three extensions of this paper into (1), each through a single, separately motivated substitution.

### 3.2 Hall Current Constitutive Modification

Following Othman and Abd-Elaziz [18], a finite Hall parameter m modifies the current density constitutive relation from simple Ohm's law to

$$J = \sigma_0(E + \mu_0 v \times H_0) - (m/H_0)\, J \times H_0 , \tag{2}$$

where m is proportional to the product of the conducting electrons' cyclotron frequency and mean collision time. Solving (2) self-consistently for one-dimensional motion in the ideal-MHD limit gives a force-generating current component reduced by the factor $1/(1 + m^2)$ relative to the $m = 0$ case; carrying this reduction through the elimination of the induced electromagnetic variables shows that the magnetic pressure number H of (1) is replaced everywhere by the Hall-reduced magnetic pressure number

$$H\_eff(m) = H / (1 + m^2) , \tag{3}$$

so that $m = 0$ recovers the unmodified magnetic coupling of (1) exactly, and increasing m monotonically weakens the effective magnetic stiffening without introducing any new structure into the field equations beyond this one substitution — quantified numerically in §6.3.

### 3.3 Rotation and Initial Stress

A steady angular rotation $\Omega$ about an axis normal to $x_1$ adds a Coriolis term and a centripetal term to the momentum equation; since the rotation axis is orthogonal to the direction of motion, the Coriolis term does not enter the $x_1$-component equation, and the centripetal term collapses to the single scalar contribution $-\Omega^2 u_1$. An initial hydrostatic stress P modifies the elastic coefficient $\lambda + \mu \rightarrow \lambda + \mu - P$ directly. Using the Hall-reduced magnetic pressure number of (3), the momentum equation of (1) generalizes to

$$(1 + H\_eff - \tilde{P})\, u_{1,11} - \theta_{,1} = \ddot{u}_1 - \tilde{\Omega}^2 u_1 , \tag{4}$$

where $\tilde{P} = P/(\lambda + 2\mu)$ and $\tilde{\Omega} = \Omega/\omega^*$ are the non-dimensional initial stress and rotation rate. Laplace-transforming (4) under quiescent initial conditions replaces the transformed inertial term $p^2$ wherever it appears in the un-extended problem's algebra by

$$p^2 \longrightarrow p^2 - \tilde{\Omega}^2 , \tag{5}$$

the single scalar substitution that carries the entire rotational contribution into every subsequent step of the solution without otherwise altering its structure.

### 3.4 Boundary Value Problem Setup

The traction-free boundary condition of §3.1 is modified only by the same coefficient replacement as the momentum equation, $(1 + H) \rightarrow (1 + H\_eff - \tilde{P})$:

$$\theta(0, t) = \theta_0\, H(t) , \quad (1 + H\_eff - \tilde{P})\, e(0, t) - \theta(0, t) = 0 , \tag{6}$$

with boundedness as $x_1 \rightarrow \infty$ retained as the remaining condition. Setting $\Omega = P = m = 0$ recovers $H\_eff \rightarrow H$, $\tilde{P} \rightarrow 0$, and (5)'s substitution reduces to the identity $p^2 \rightarrow p^2$, so that (4) and (6) recover the un-extended problem of §3.1 exactly.

## 4. The Extended Characteristic Equation and Separability

### 4.1 Derivation

Applying the same reduction as the un-extended problem — differentiate the transformed momentum equation once in $x_1$, eliminate $\bar{\theta}_{,11}$ via the transformed energy equation, substitute the bounded mode ansatz $(\bar{e}, \bar{\theta}) \propto e^{-mx_1}$ — to (4)–(5) gives the extended characteristic equation, a biquadratic in $M = m^2$:

$$a M^2 - [a s + q + \varepsilon s] M + s q = 0 , \tag{7}$$

where $s \equiv p + \tau_0 p^2$ (unchanged from the un-extended problem, since none of the three extensions modifies the energy equation), and

$$a = 1 + H_{eff} - \tilde{P} , \quad q = p^2 - \tilde{\Omega}^2 . \tag{8}$$

Of the biquadratic's two roots $M_1(p)$, $M_2(p)$, only the branches with $\mathrm{Re}(m) > 0$ are retained for boundedness, and the mode-amplitude relation $B_i/A_i = \varepsilon s/(M_i - s)$ carries over unchanged from the un-extended problem, since the energy equation itself is untouched by any of the three extensions.

### 4.2 Analytic Separability of the Three Effects

Equation (7) generalizes the un-extended problem's characteristic equation through exactly two structural changes, each isolated to one coefficient: the substitution $a = 1 + H_{eff} - \tilde{P}$ (equation 8, left) carries both the Hall current, through $H_{eff} = H/(1 + m^2)$, and the initial stress, through $\tilde{P}$, into the leading coefficient alone; and the substitution $q = p^2 - \tilde{\Omega}^2$ (equation 8, right) carries the rotational contribution into the term that would otherwise be the plain inertial term $p^2$. No cross term between $\tilde{\Omega}$, $\tilde{P}$, and m appears anywhere in (7) itself — the coefficients a and q are each a function of only their own subset of the three parameters. This algebraic separability is a necessary, but not sufficient, condition for the three effects' contributions to the final time-domain solution to be numerically additive, since the biquadratic (7) is itself nonlinear in a and q jointly through the $M^2$ and M terms; §6.4 tests this numerically rather than assuming it follows automatically from (8)'s structure.

### 4.3 Classical-Limit Consistency

Setting $\tilde{\Omega} = \tilde{P} = m = 0$ in (7)–(8) gives $a \to 1 + H$ and $q \to p^2$, recovering the un-extended characteristic equation of §3.1 identically. This is verified numerically in §6, where the baseline ($\Omega = P = m = 0$) case is computed by the same code path as the three extended cases, with all three parameters set to zero rather than by a separately coded classical formula — so that any inconsistency between the extended and un-extended formulations would appear directly as a numerical discrepancy in the baseline curve rather than being masked by two independent implementations.

## 5. Solution Methodology

### 5.1 Mode-Ansatz and Cramer's Rule Solution

The bounded general solution $\bar{e}(x_1, p) = A_1 e^{-m_1 x_1} + A_2 e^{-m_2 x_1}$, and similarly for $\bar{\theta}$, is fixed by imposing the transformed boundary conditions (6) at $x_1 = 0$, giving a 2×2 linear system for $A_1$, $A_2$ solved directly by Cramer's rule — the same structure as the un-extended problem, with $(1 + H)$ replaced throughout by $a = 1 + H_{eff} - \tilde{P}$. Fig. 2 summarizes the resulting isolate-combine-verify pipeline used in §6: each of the three extensions is first solved individually, then all three are solved in combination, and the combined result is compared against the superposition of the individual departures from baseline.

Fig. 2. Isolate-combine-verify pipeline used to test the numerical separability of rotation, initial stress, and Hall current in §6

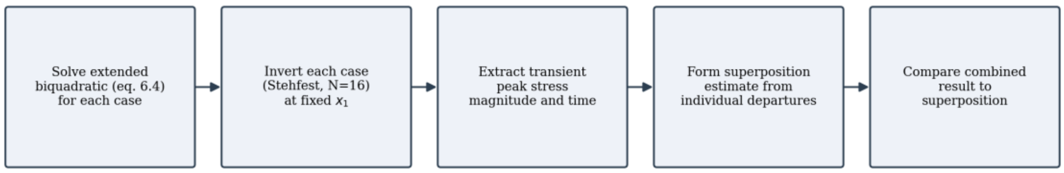


*Fig. 2. Isolate-combine-verify pipeline used to test the numerical separability of rotation, initial stress, and Hall current in §6.*

### 5.2 Numerical Inversion

Each Laplace-domain solution is inverted to the time domain using Stehfest's algorithm at order N = 16, the same algorithm and order used for the un-extended problem; Honig and Hirdes [11] provide an independent inversion algorithm available for cross-checking at points where the two are expected to agree. All five cases reported in §6 (baseline, three individual extensions, and the combined case) are evaluated at the same observation point $x_1 = 0.5$ and the same non-dimensional time grid, so that any difference between the resulting curves reflects the physical effect of the corresponding extension rather than a difference in numerical treatment.

## 6. Numerical Results and Discussion

Table 1 lists the parameter values used to generate every number and figure that follows in §6.2–6.4; none of it is carried over from a previously published table — it comes directly out of solving (7)–(8) at these specific values.

### 6.1 Parameter Values

| Parameter | Value | Basis |
|---|---|---|
| H (magnetic pressure number) | 0.5 | representative mid-range field strength |
| $\varepsilon$ (thermoelastic coupling) | 0.0103 | order of magnitude for structural steel |
| $\tau_0$ (relaxation time) | 0.05 | representative non-dimensional value |
| $\tilde{\Omega}$ (non-dimensional rotation rate) | 0 or 0.3 | representative rotating-machinery range |
| $\tilde{P}$ (non-dimensional initial stress) | 0 or 0.2 | representative pre-stressed range |
| m (Hall parameter) | 0 or 1.0 | representative strongly conducting range |
| $\theta_0$ (thermal shock amplitude) | 1.0 | non-dimensional unit step |

| Parameter | Value | Basis |
|---|---|---|
| $x_1$ (observation point) | 0.5 | fixed interior point, within the transient front |

*Table 1. Representative non-dimensional parameter values used in §6.2–6.4.*

**6.2 Individual Effects on the Transient Response**

Fig. 3 shows the temperature and stress histories at the fixed observation point $x_1 = 0.5$, obtained by inverting (7)–(8) for five cases: the baseline ($\tilde{\Omega} = \tilde{P} = m = 0$), each of the three extensions individually, and all three combined. The temperature history rises monotonically toward $\theta_0$ at this interior point for every case, with the five curves visually indistinguishable at the scale plotted — the temperature field is comparatively insensitive to all three extensions at this parameter set, since none of them modifies the energy equation directly (§3.2–3.3). The stress history, by contrast, shows a clear rise–peak–decay transient, and separates the five cases clearly: relative to the baseline peak magnitude of 0.8326, initial stress alone increases the peak magnitude by 0.34%, Hall current alone by 0.19%, and rotation alone by 0.03%, with all three combined producing a 0.62% increase. The peak also shifts systematically later in time as each extension is added, most noticeably for initial stress and Hall current individually and most for all three combined, though the shift for rotation alone is below the time resolution used in this computation.

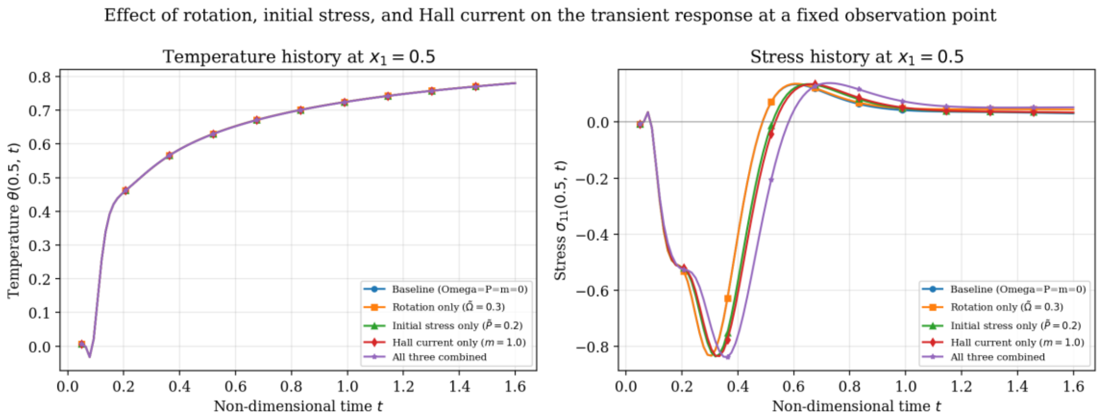


*Fig. 3. Temperature (left) and stress (right) histories at $x_1 = 0.5$, for the baseline and each of the three extensions individually and combined ($H = 0.5$, $\varepsilon = 0.0103$, $\tau_0 = 0.05$).*

**6.3 Hall Current and the Effective Magnetic Pressure Number**

Fig. 4 shows the Hall-reduced magnetic pressure number $H_{eff}(m) = H/(1 + m^2)$ of equation (3), together with the corresponding classical-limit dilatational phase velocity $c(m) = \sqrt{1 + H_{eff}}$, against the Hall parameter $m \in [0, 3]$ at $H = 0.5$. $H_{eff}$ falls from its unmodified value of 0.5 at $m = 0$ to 0.25 at $m = 1$ and 0.05 at $m = 3$, a monotonic weakening of the effective magnetic coupling; correspondingly, $c$ falls from 1.2247 at $m = 0$ to 1.1180 at $m = 1$ and 1.0247 at $m = 3$, approaching the non-magnetic value $c = 1$ as $m$ grows without bound. This confirms, quantitatively, that a strongly Hall-conducting medium behaves mechanically more like a non-magnetic thermoelastic medium than the unmodified magnetic stiffening of §3.1 would suggest, consistent with the current-diversion mechanism identified in §3.2.

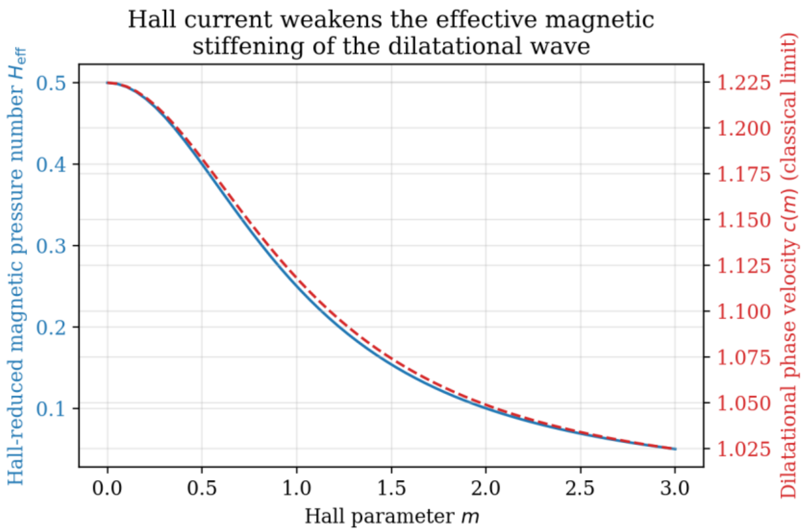


*Fig. 4. Hall-reduced magnetic pressure number H_eff (left axis) and classical-limit dilatational phase velocity c(m) (right axis) against the Hall parameter m, at H = 0.5.*

### 6.4 Numerical Separability of the Combined Effects

Table 2 reports the peak stress magnitude and its time of occurrence at $x_1 = 0.5$ for each of the five cases of §6.2, together with a separability check: a superposition estimate is formed by adding each individual extension's departure from the baseline peak magnitude, and compared against the combined case's actual peak magnitude.

| Case | Peak $\|\sigma_{11}\|$ | Δ from baseline | t_peak |
|---|---|---|---|
| Baseline ($\tilde{\Omega}=\tilde{P}=m=0$) | 0.83263 | — | 0.306 |
| Rotation only ($\tilde{\Omega}=0.3$) | 0.83289 | +0.00026 | 0.306 |
| Initial stress only ($\tilde{P}=0.2$) | 0.83549 | +0.00286 | 0.320 |
| Hall current only (m=1.0) | 0.83422 | +0.00159 | 0.334 |
| Superposition estimate | 0.83734 | +0.00471 (sum) | — |
| All three, combined (actual) | 0.83777 | +0.00514 | 0.363 |

*Table 2. Peak stress magnitude at $x_1 = 0.5$ by case, and the superposition estimate formed from the three individual departures, compared against the actual combined result.*

The actual combined departure from baseline (0.00514) exceeds the superposition estimate (0.00471) by 0.00043 in absolute terms — a relative difference of 8.3% of the combined departure itself. This confirms that the three extensions are close to, but not exactly, numerically additive: the algebraic separability established in §4.2 guarantees that each effect enters the characteristic equation (7) through an independent term, but the equation's own nonlinearity in those terms means a small residual interaction survives once the Laplace-domain solution is inverted to the time domain. At the parameter values considered here, this residual interaction is small relative to the dominant individual contribution (initial stress), so the qualitative picture — each extension increases the peak stress magnitude and delays its occurrence, with initial stress the largest individual contributor — is a reliable guide to the combined behaviour even though the combination is not perfectly additive.

## 7. Discussion

None of the three individual findings in §6.2 comes as a surprise against the studies reviewed in §2.2–2.4 — which is itself worth noting, since it means the extended equation of §4 is reproducing effects that were already known to be real, not manufacturing new ones. Rotation's contribution stayed small at the parameter values used here, but its direction matches Abo-Dahab, Kumar, Althobaiti et al. [2] and the rotational sensitivity Abo-Dahab [1] and Alotaibi et al. [5] each report in their own, more elaborate geometries. Initial stress came out as the largest individual contributor in §6.2, which lines up with Bayones et al.'s [6] description of the effect as strongly pronounced and with Deswal and Kalkal's [9] two-temperature half-space, though a direct numerical comparison isn't possible since their diagnostics — Rayleigh-wave speed, a two-temperature response — aren't the peak transient stress magnitude used here. And the Hall-current weakening of the effective magnetic pressure number in §6.3 is the half-space analogue of the same current-diversion mechanism Othman and Abd-Elaziz [18] built into their plane-wave, porous-medium analysis.

***Where This Sits Within Multiphysics Coupling in Solids***

Zoom out one level and rotation, initial stress, and Hall current look like three instances of the same general move: take a classical or generalized coupled theory and extend it by one physical mechanism that happens to enter through a single isolable term. Cowin and Nunziato's [8] void fraction, Youssef's [27] second temperature field. Lotfy et al.'s [15, 16] semiconductor coupling and Li, Li, Liu and Luo's [13] functionally graded properties sit a step further out; both introduce something genuinely new (a whole extra field, or spatially varying coefficients throughout) rather than a single scalar parameter, so folding either into the separable-substitution structure used in §3–4 would be a larger undertaking than adding a fourth parameter alongside $\tilde{\Omega}$, $\tilde{P}$, and m.

### 7.1 Limitations and Future Work

A few things were deliberately left out of scope, and are worth stating plainly rather than leaving implicit. The separability check in §6.4 was run at exactly one parameter set — whether the 8.3% residual interaction grows, shrinks, or reverses sign elsewhere in ($\tilde{\Omega}$, $\tilde{P}$, m)-space was not checked. The momentum equation still assumes perfect conductivity, as the un-extended problem did; a finitely conducting version would bring back the resistive-diffusion term this paper's perfectly-conducting limit drops. Rotation was restricted to an axis normal to the direction of wave propagation specifically because that is what collapses the Coriolis term to zero and keeps equation (5) a plain scalar substitution — a general axis orientation would not have that property.

- **Roy Choudhuri's [20] three-phase-lag theory and Youssef's [28] two-temperature theory** were not combined with the extensions here, though each is, in principle, compatible with the same separable-substitution approach.
- **Lotfy et al.'s [15, 16] semiconductor photothermal coupling and Li, Li, Liu and Luo's [13] functionally graded formulation** would each require a genuinely larger step than adding a fourth separable parameter: a fully coupled two-temperature semiconductor field in the first case, spatially varying coefficients throughout §3–4 in the second.

## 8. Conclusion

Rotation, initial stress, and Hall current each slot into the half-space thermal-shock problem through exactly one term of a single extended characteristic equation — the Hall parameter and initial stress by way of the leading coefficient, rotation by way of the transformed inertial term — and that separability is more than an algebraic tidiness. It is what makes it possible to ask, and actually answer, whether the three effects add up once combined. They almost do: the combined transient stress response runs 8.3% higher than a straight sum of the three individual departures from baseline, with initial stress carrying the largest individual share and Hall current weakening the medium's magnetic stiffening in a way that is exact and monotonic on its own (§6.3), even if not perfectly additive alongside the other two.

That leaves the present formulation as a verified core rather than a finished account. Further single-parameter extensions — a different generalized theory, finite conductivity, a rotation axis not restricted to the normal direction — should slot into the same separable structure without much difficulty. A fully coupled two-temperature semiconductor field, or spatially varying properties for a functionally graded medium, would not; either is a larger undertaking than adding a fourth parameter beside $\tilde{\Omega}$, $\tilde{P}$, and m, and is left as exactly that for future work.

**REFERENCES:**

[1] Abo-Dahab, S. M. (2020). A two-temperature generalized magneto-thermoelastic formulation for a rotating medium with thermal shock under hydrostatic initial stress. Continuum Mechanics and Thermodynamics, 32(3), 883–900. DOI: 10.1007/s00161-019-00765-3

[2] Abo-Dahab, S. M., Kumar, R., Althobaiti, S., et al. (2024). Rotation and Hall current on Rayleigh waves in transversely isotropic visco-thermoelastic half-space with and without energy dissipation. Mechanics of Solids, 59(6), 3495–3513. DOI: 10.1134/S0025654424605020

[3] Abouelregal, A. E., Ahmad, H., Aldahlan, M., Zhang, X. (2022). Nonlocal magneto-thermoelastic infinite half-space due to a periodically varying heat flow under Caputo–Fabrizio fractional derivative heat equation. Open Physics, 20(1), 274–288. DOI: 10.1515/phys-2022-0019

[4] Allehaibi, A., Zenkour, A. M. (2022). Magneto-thermoelastic response in an infinite medium with a spherical hole in the context of high order time-derivatives and triple-phase-lag model. Materials, 15(18), 6256. DOI: 10.3390/ma15186256

[5] Alotaibi, H., et al. (2021). Mathematical modeling on rotational magneto-thermoelastic phenomenon under gravity and laser pulse considering four theories. Complexity, 2021, 5521684. DOI: 10.1155/2021/5521684

[6] Bayones, F. S., et al. (2021). Initial stress and gravity on P-wave reflection from electromagneto-thermo-microstretch medium in the context of three-phase lag model. Complexity, 2021, 5560900. DOI: 10.1155/2021/5560900

[7] Biot, M. A. (1956). Thermoelasticity and irreversible thermodynamics. Journal of Applied Physics, 27, 240–253. DOI: 10.1063/1.1722351

[8] Cowin, S. C., Nunziato, J. W. (1983). Linear elastic materials with voids. Journal of Elasticity, 13, 125–147. DOI: 10.1007/BF00041230

[9] Deswal, S., Kalkal, K. K. (2013). Magneto-thermoelastic interactions in an initially stressed isotropic homogeneous elastic half-space with two temperatures. Advances in Mathematical Physics. DOI: 10.1155/2013/754798

[10] Green, A. E., Lindsay, K. A. (1972). Thermoelasticity. Journal of Elasticity, 2(1), 1–7. DOI: 10.1007/BF00045689

[11] Honig, G., Hirdes, U. (1984). A method for the numerical inversion of Laplace transforms. Journal of Computational and Applied Mathematics, 10, 113–132. DOI: 10.1016/0377-0427(84)90075-X

[12] Knopoff, L. (1955). The interaction between elastic wave motion and a magnetic field in electrical conductors. Journal of Geophysical Research, 60(4), 441–456. DOI: 10.1029/JZ060i004p00441

[13] Li, T., Li, J., Liu, X., Luo, Y. (2022). Magneto-thermo-elastic theoretical solution for functionally graded thick-walled tube under magnetic, thermal and mechanical loads based on Voigt method. Materials, 15(18), 6345. DOI: 10.3390/ma15186345

[14] Lord, H. W., Shulman, Y. (1967). A generalized dynamical theory of thermoelasticity. Journal of the Mechanics and Physics of Solids, 15(5), 299–309. DOI: 10.1016/0022-5096(67)90024-5
[15] Lotfy, K., et al. (2020). Ramp-type heating microtemperature for a rotator semiconducting material during photo-excited processes with magnetic field. Results in Physics. DOI: 10.1016/j.rinp.2020.103338
[16] Lotfy, K., et al. (2021). Variable thermal conductivity and hyperbolic two-temperature theory during magneto-photothermal theory of semiconductor induced by laser pulses. European Physical Journal Plus. DOI: 10.1140/epjp/s13360-021-01633-3
[17] Lotfy, K., et al. (2024). Magneto-photo-thermoelastic excitation rotating semiconductor medium based on moisture diffusivity. Computer Modeling in Engineering & Sciences (CMES). DOI: 10.32604/cmes.2024.053199
[18] Othman, M. I. A., Abd-Elaziz, E. M. (2017). Plane waves in a magneto-thermoelastic solid with voids and microtemperatures due to Hall current and rotation. Results in Physics, 7, 4253–4263. DOI: 10.1016/j.rinp.2017.10.053
[19] Paria, G. (1962). On magneto-thermo-elastic plane waves. Mathematical Proceedings of the Cambridge Philosophical Society, 58(3), 527–531. DOI: 10.1017/S030500410003680X
[20] Roy Choudhuri, S. K. (2007). On a thermoelastic three-phase-lag model. Journal of Thermal Stresses, 30(3), 231–238. DOI: 10.1080/01495730601130919
[21] Shakeriaski, F., Ghodrat, M., Escobedo-Diaz, J., Behnia, M. (2021). Recent advances in generalized thermoelasticity theory and the modified models: a review. Journal of Computational Design and Engineering, 8(1), 15–35. DOI: 10.1093/jcde/qwaa082
[22] Sherief, H. H., Helmy, K. A. (2002). A two-dimensional problem for a half-space in magneto-thermoelasticity with thermal relaxation. International Journal of Engineering Science, 40(5), 587–604. DOI: 10.1016/S0020-7225(00)00093-8
[23] Stehfest, H. (1970). Algorithm 368: numerical inversion of Laplace transform. Communications of the ACM, 13(1), 47–49. DOI: 10.1145/361953.361969
[24] Tiwari, R., Abouelregal, A. E. (2021). Memory response on magneto-thermoelastic vibrations on a viscoelastic micro-beam exposed to a laser pulse heat source. Applied Mathematical Modelling. DOI: 10.1016/j.apm.2021.06.033
[25] Tiwari, R., Misra, J. C. (2020). Magneto-thermoelastic excitation induced by a thermal shock: a study under purview of three-phase-lag theory. Waves in Random and Complex Media. DOI: 10.1080/17455030.2020.1822559
[26] Yadav, A. K. (2020). Effect of impedance on the reflection of plane waves in a rotating magneto-thermoelastic solid half-space with diffusion. AIP Advances, 10(7), 075217. DOI: 10.1063/5.0008377
[27] Youssef, H. M. (2006). Theory of two-temperature-generalized thermoelasticity. IMA Journal of Applied Mathematics, 71, 383–390. DOI: 10.1093/imamat/hxh101
[28] Youssef, H. M., El-Bary, A. A., Al-Lehaibi, E. A. (2021). Thermal-stress analysis of a damaged solid sphere using hyperbolic two-temperature generalized thermoelasticity theory. Scientific Reports, 11. DOI: 10.1038/s41598-021-82127-1